Electronic Supplementary Material (ESI) for Physical Chemistry Chemical Physics.

Electronic Supporting Information

TICT Compounds by Design: Comparison of two Naphthalimide-π-Dimethylaniline Conjugates of Different Length and Ground State Geometry

Justina Jovaišaitė,[a*] Paulius Baronas,[a] Gediminas Jonusauskas,[b] Dalius Gudeika,[c] Alytis Gruodis,[d] Juozas V. Gražulevičius[c] and Saulius Juršėnas[a]

[a] Institute of Photonics and Nanotechnology, Vilnius University, Saulėtekio Ave. 3, LT-10257 Vilnius, Lithuania Email: justina.jovaisaite@ff.vu.lt

[b] Laboratoire Ondes et Matière d'Aquitaine, Bordeaux University, UMR CNRS 5798, 351 cours de la Libération, 33405 Talence, France

[c] Department of Polymer Chemistry and Technology, Kaunas University of Technology, Radvilėnų rd. 19, LT-50254 Kaunas, Lithuania

[d] Institute of Chemical Physics, Vilnius University, Saulėtekio Ave. 3, LT-10257 Vilnius, Lithuania

Table of Contents

Synthesis and Materials

The synthesis of 4-bromo-*N*-(2-ethylhexyl)-1,8-naphthalimide was published elsewhere.[1]

4-(4-(Dimethylamino)phenyl)-*N*-(2-ethylhexyl)-1,8-naphthalimide (**NA1**). To a degassed solution of the 4-bromo-*N*-(2-ethylhexyl)-1,8-naphthalimide (0.5 g, 1.29 mmol) and $Pd(PPh_3)_2Cl_2$ (0.03 g, 0.04 mmol) in THF (15 mL), a solution of 4-(4,4,5,5-tetramethyl[1,3,2]dioxaborolan-2-yl)-*N,N*-dimethylaniline (0.38 g, 1.55 mmol) in THF (3 mL) and aqueous K_2CO_3 solution (1.79 g, 12.89 mmol) in H_2O (2 mL) were added *via* a syringe. The reaction mixture was stirred at 80 °C for 24 h. After cooling down, the product was extracted with CH_2Cl_2, washed with water and dried over $MgSO_4$. The crude product was purified by silica gel column chromatography eluted with ethyl acetate and hexane (1:10, *V:V*), recrystallized from eluent to obtain NA1 as a yellow crystals. Yield: 0.35 g (64%), m.p. 142-143 °C; ^{1}H NMR spectrum (300 MHz, $CDCl_3$, δ, ppm): 8.65 (d, J = 1.1 Hz, 1H), 8.63 (d, J = 1.1 Hz, 1H), 8.44 (d, J = 8.5 Hz, 1H), 7.75-7.67 (m, 2H), 7.45 (d, J = 8.5 Hz, 2H), 6.90 (d, J = 8.5 Hz, 2H), 4.24-4.12 (m, 2H), 3.09 (s, 6H), 2.03-1.94 (m, 1H), 1.49-1.27 (m, 8H), 1.01-0.87 (m, 6H). ^{13}C NMR spectrum (75.4 MHz, CDCl3, δ, ppm): 164.8, 150.5, 147.5, 146.3, 144.0, 133.0, 130.6, 130.1, 129.0, 128.2, 127.4, 126.4, 122.9, 120.6, 112.2, 44.1, 40.4, 37.9, 30.8, 28.7, 24.1, 23.1, 14.1, 10.7. IR, (in KBr), cm^{-1}: 3045 ν (CH_{ar}); 2949, 2898 ν ($CH_{aliphatic}$); 1688 ν ($C=O_{anhydride}$); 1655, 1591 ν ($C=C_{ar}$); 1388, 1357 ν (C-N); 775, 716 γ (CH_{ar}). MS ($APCI^+$, 20 V), m/z: 429 ($[M+H]^+$). Anal. Calcd. for $C_{28}H_{32}N_2O_2$: C, 78.47; H, 7.53, N, 6.54; O, 7.47%; found C 78.39, H 7.61, N 6.51%.

4-((4-(Dimethylamino)phenyl)ethynyl)-N-(2-ethylhexyl)-1,8-naphthalimide (**NA2**). A mixture of 4-bromo-*N*-(2-ethylhexyl)-1,8-naphthalimide (0.5 g, 1.29 mmol), 4-ethynyl-*N,N*-dimethylaniline (0.26 g, 1.80 mmol), $Pd(PPh_3)_2Cl_2$ (0.009 g, 0.01 mmol), CuI (0.007 g, 0.04 mmol), triphenylphosphine (0.007 g, 0.03 mmol), and triethylamine (15 mL) was heated under reflux for 24 h. After removal of the solvent the residue was adsorbed on

silica gel and purified by column chromatography eluting with a mixture of hexane and ethyl acetate (9:1, *V:V*) and then recrystallized from eluent to yield 0.32 g (55%) of orange crystals (m.p. 164-165 ^{o}C). ^{1}H NMR spectrum (300 MHz, $CDCl_3$, δ, ppm): 8.74 (d, J = 8.3 Hz, 1H), 8.62 (d, J = 7.6 Hz, 1H), 8.52 (d, J = 7.6 Hz, 1H), 7.87 (d, J = 7.6 Hz, 1H), 7.81 (t, J = 7.6 Hz, 1H), 7.55 (d, J = 8.3 Hz, 2H), 6.73 (d, J = 8.3 Hz, 2H), 4.18-4.05 (m, 2H), 3.06 (s, 6H), 2.01-1.91 (m, 1H), 1.45-1.24 (m, 8H), 0.99-0.85 (m, 6H). ^{13}C NMR spectrum (75.4 MHz, $CDCl_3$, δ, ppm): 164.5, 164.2, 150.6, 133.6, 133.3, 132.5, 131.4, 131.3, 130.6, 129.8, 128.7, 128.1, 127.0, 122.8, 120.9, 111.8, 101.6, 85.3, 77.3, 77.0, 76.7, 44.1, 40.2, 37.9, 30.7, 28.7, 24.0, 23.1, 14.1, 10.6. IR, (in KBr), cm^{-1}: 3029 ν (CH_{ar}); 2928, 2919, 2844 ν ($CH_{aliphatic}$); 2199 ν ($C_{ar}{\equiv}C_{ar}$); 1703 ν ($C{=}O_{anhydride}$); 1665, 1604, 1442 ν ($C{=}C_{ar}$); 1383, 1335, 1241 ν (C-N); 851, 782, 728, 677 γ (CH_{ar}). MS (APCI^{+}, 20 V), m/z: 453 ([M+H]$^{+}$). Anal. Calcd. for $C_{30}H_{32}N_2O_2$: C, 79.61; H, 7.13, N, 6.19; O, 7.07%; found C 79.59, H 7.11, N 6.11%.

General methods for experiments

The solvents used in photophysical experiments cyclohexane (CyHex), toluene (TOL), diethyl ether (DEE), chloroform (CHL), ethyl acetate (EA), dimethoxyethane (DME), dichloromethane (DCM), acetone (AC), acetonitrile (ACN) were of spectroscopic grade (Sigma-Aldrich). Cells of 1 cm for steady-state and time resolved fluorescence measurements were used, 2 mm cells were utilised for femtosecond transient absorption measurements.

Thin film samples were prepared by drop casting the compound/polymer mixture on quartz plates:

1) **NA1** and **NA2** in 1 wt% polystyrene (PS);
2) **NA1** and **NA2** in 1 wt% poly(methyl methacrylate) (PMMA);
3) **NA1** and **NA2** in 1 wt% PMMA with 20 wt% of camphoric anhydrite (PMMA/CA).

Polymers and camphoric anhydrite were purchased from Sigma-Aldrich and used as received.

Steady-state spectroscopy

The absorption spectra were taken on a Varian-Cary 5G spectrophotometer. The fluorescence spectra measurements were performed using a FluoroMax-3 spectrofluorometer. Spectral measurements were carried out in air-saturated solutions at room temperature; the concentrations of the studied compounds for absorption and fluorescence spectra measurements were $5x10^{-6}$ M. All measured fluorescence spectra were corrected for nonuniformity of detector spectral sensitivity.

Fluorescence quantum yields for solutions were determined by comparative method. The concentrations of studied compounds in CyHex, DEE, DME and EA together with relative standard 9,10-diphenylanthracene in CyHex ($\boldsymbol{\varphi^{fl} = 0.97}$)[2] were selected so that OD would be around 0.05. The fluorescence quantum yields were calculated using:

$$\varphi_s^{fl} = \varphi_0^{fl} \frac{S_s A_0 n_s^2}{S_0 A_s n_0^2}. \quad (1)$$

For **NA1** and **NA2** in AC and ACN, $Ru(bpy)_3^{2+}$ in H_2O ($\boldsymbol{\varphi^{fl} = 0.04}$)[2] were used as a standard and the concentrations were made so that OD would be around 0.1. The following formula for quantum yield determination was employed:

$$\varphi_s^{fl} = \varphi_0^{fl} \frac{S_s(1-10^{-A_0})n_s^2}{S_0(1-10^{-A_s})n_0^2}. \quad (2)$$

Where $\boldsymbol{\varphi_s^{fl}}$ and $\boldsymbol{\varphi_0^{fl}}$ are the fluorescence quantum yields of the studied samples in solvents and the standard compound as reference, respectively; $\boldsymbol{A_s}$ and $\boldsymbol{A_0}$ are the OD of samples and standard reference compounds, respectively; $\boldsymbol{S_s}$ and $\boldsymbol{S_0}$ denotes areas underneath the curves of the fluorescence spectra of the sample solution and the standard reference, respectively; and $\boldsymbol{n_s}$ and $\boldsymbol{n_0}$ are the refraction indices of solvents for the substance under study and the standard compound.

Fluorescence quantum yields for films were determined by using integrated sphere.

Weller's polarity plot

Weller's equation is a modified version of the Lippert–Mataga equation to estimate the excited state dipole moments.[3]

$$\vartheta_{FL} = -\frac{2}{hc}\mu_e^2 a^{-3}\Delta f' + const. \quad (3)$$

In the above equation ϑ_{FL} is a wavenumber of fluorescence spectra maxima; μ_e is the excited state dipole moment; h is a Planck constant; c – velocity of light; a – Onsager cavity radius, $\Delta f'$ is a solvent-dependent parameter that includes solvent's dielectric constant, ε, and refractive index, n:

$$\Delta f' = \frac{\varepsilon-1}{2\varepsilon+1} - \frac{n^2-1}{4n^2+2}. \quad (4)$$

The Onsager cavity radius (a=5.67 Å for **NA1** and a=5.99 Å for **NA2**) was obtained as half of the distances between the carbonyl oxygen and amino nitrogen from the optimized ground state geometry.[4]

The excited state dipole moment is then obtained as follows:

$$\mu_e = \sqrt{-\frac{1}{2}\frac{\vartheta_{FL}}{\Delta f} hca^3}. \quad (5)$$

Where $\frac{\vartheta_{FL}}{\Delta f}$ is a slope, obtained from a linear fit, by plotting ϑ_{FL}vs. $\Delta f'$.

Time-resolved spectroscopy

Fluorescence lifetimes were obtained by using depolarized excitation light. The highest pulse energies used to excite fluorescence did not exceed 100 nJ and the average power of the excitation beam was 0.1 mW at a pulse repetition rate of 1 kHz focused onto a spot with a diameter of 0.1 mm in the 10 mm-long fused-silica cell. The fluorescence emitted in the forward direction was collected by reflective optics and focused with a

spherical mirror onto the input slit of a spectrograph (Chromex 250) coupled to a streak camera (Hamamatsu 5680 equipped with a fast single sweep unit M5676, temporal resolution 2 ps). Convolution of a rectangular streak camera slit in the sweep range of 250 ps with electronic jitter of the streak camera trigger pulse provided a Gaussian (over four decades) temporal apparatus function with a full width at half-maximum of 20 ps.

Femtosecond time-resolved differential absorption (TA) measurements were performed using a Harpia pump-probe spectrometer (Light Conversion) pumped with a 10 kHz pulsed laser Pharos-SP (Light Conversion). The probe source was white light continuum generated by focusing 190 fs 1030 nm laser pulses onto a sapphire crystal. Pump wavelength was set to 420 nm using an optical parametric amplifier Orpheus (Light Conversion).

Global analysis

Global analysis of TA data was performed by data analysis software "CarpetView" (Light Conversion). A sequential model was employed including three (or four) excited states up to 16 ps (or 10 ps) for **NA1** (or **NA2**).

Computational details

Quantum chemical calculations of studied derivatives were performed using DFT and TD-DFT implemented in the *Gaussian 16*[5] software package. Geometry optimization was provided by means of density functional CAM-B3LYP method and 6-31g(d,p) basis set in the ground S_0 state as well as the lowest excited S_1 state. Solvent surrounding (cyclohexane, acetonitrile) was simulated using PCM method.

The evaluation of the twisted excited states was carried on with semi-empirical MOPAC, using PM7 Hamiltonian, including solvent with COSMO model.[6]

Results

Computational data

Table S1. Calculated dihedral angles in the ground and excited state geometries of **NA1** and **NA2** and energies of electronic transitions $S_0 \rightarrow S_1$ and $S_1 \rightarrow S_0$ in different solvents.

Compound	Solvent	Ground state		Excited state		$S_0 \rightarrow S_1$,	$S_1 \rightarrow S_0$,
		ϕ_1[1]	ϕ_2[2]	ϕ_1[3]	ϕ_2[3]	eV	eV
NA1	CyHex	7.32	53.14	0.2	33.97	3.48	2.87
	ACN	7.35	51.88	0.97	31.51	3.35	2.57
NA2	CyHex	1.33	0.92	0.74	0.48	3.15	2.69
	ACN	0.16	0.43	0.25	0.49	3.07	2.38

[1] ϕ_1 denotes angle between dimethylamine and benzene ring.

[2] ϕ_2 denotes angle between naphthalimide unite and benzene ring.

[3] Angles between dimethylamine and benzene ring (φ_1) and between naphthalimide unite and benzene ring (ϕ_2) in the excited state geometry. For the comment on the obtained values, see text below Table S1.

The optimisation of the potential surface of the lowest excited singlet when varying the twist angle was not successful with selected long-range separated functional CAM-B3LYP and PCM solvent model, i.e., no significant twist was obtained in acetonitrile and the calculated transition energies ($S_1 \rightarrow S_0$) reassembles only the blue fluorescence spectra band. On the other hand, the semi-empirical evaluation with PM7 Hamiltonian of MOPAC (with solvent model COSMO) allowed to reproduce the twisted geometries of NI compounds in most polar environment, as showed in Figure S1.

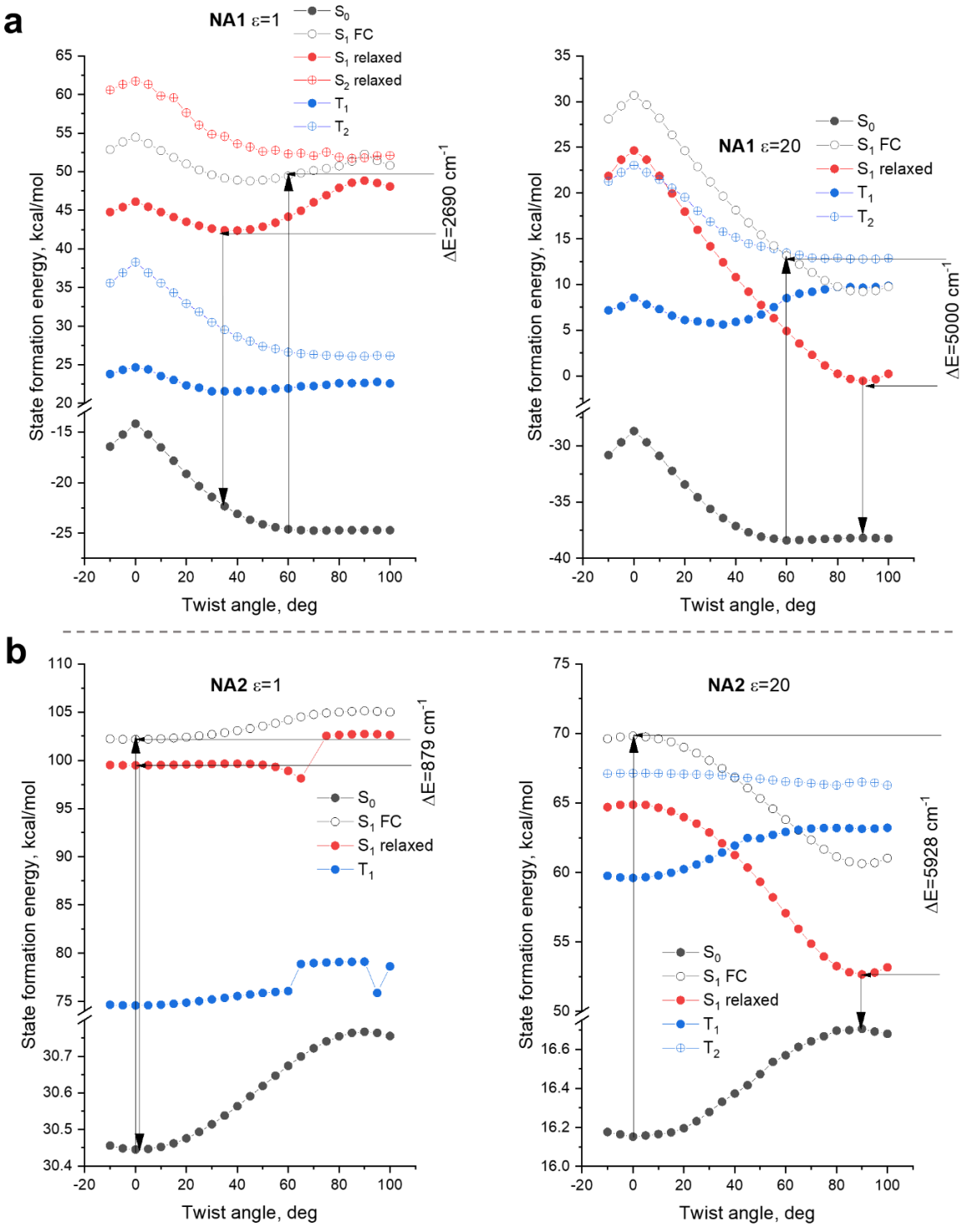

Figure S1. Potential energy surfaces versus twist angle between naphthalimide unit and dimethylaniline for **NA1** (a) and **NA2** (b) in non-polar (with ε=1) and polar (with ε=20) environments, obtained with semi-empirical method (PM7 Hamiltonian of MOPAC, solvent model COSMO).

Table S2. The calculated ground state dipole moments.

Compound	Solvent	μ, D
NA1	CyHex	8.5
	ACN	9.6
NA2	CyHex	11.3
	ACN	9.9

Photophysical data

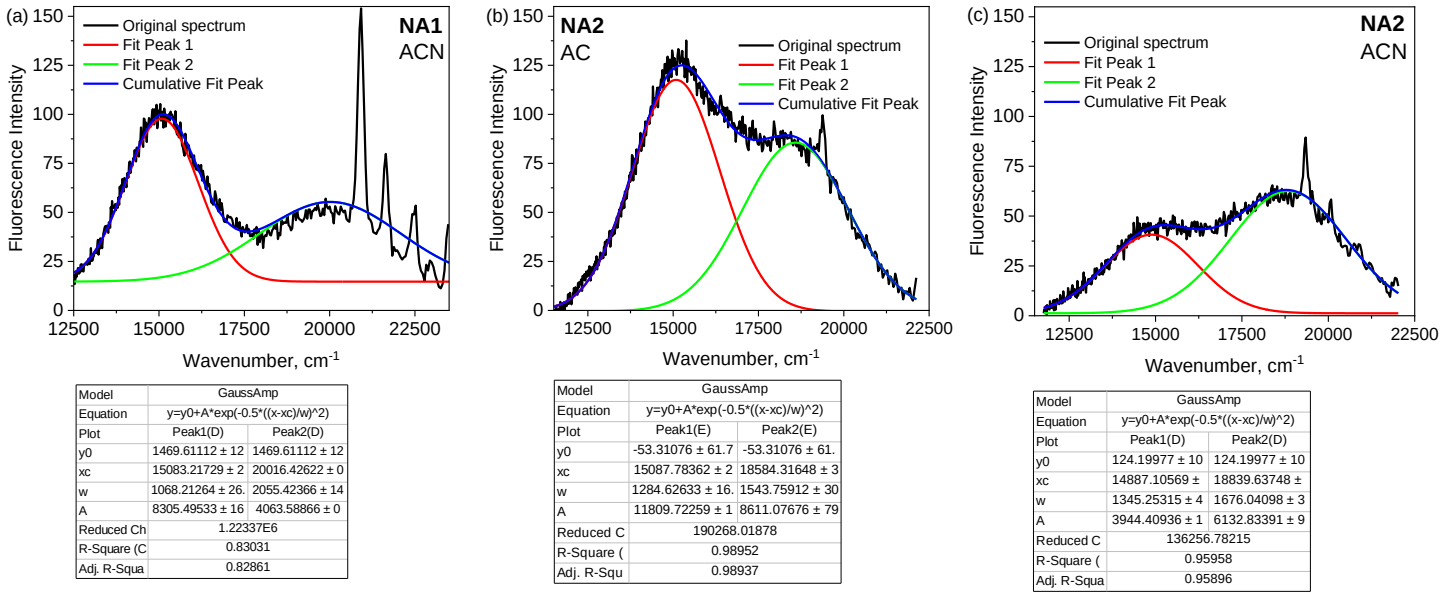

Model	GaussAmp	
Equation	y=y0+A*exp(-0.5*((x-xc)/w)^2)	
Plot	Peak1(D)	Peak2(D)
y0	1469.61112 ± 12	1469.61112 ± 12
xc	15083.21729 ± 2	20016.42622 ± 0
w	1068.21264 ± 26.	2055.42366 ± 14
A	8305.49533 ± 16	4063.58866 ± 0
Reduced Ch	1.22337E6	
R-Square (C	0.83031	
Adj. R-Squa	0.82861	

Model	GaussAmp	
Equation	y=y0+A*exp(-0.5*((x-xc)/w)^2)	
Plot	Peak1(E)	Peak2(E)
y0	-53.31076 ± 61.7	-53.31076 ± 61.
xc	15087.78362 ± 2	18584.31648 ± 3
w	1284.62633 ± 16.	1543.75912 ± 30
A	11809.72259 ± 1	8611.07676 ± 79
Reduced C	190268.01878	
R-Square (	0.98952	
Adj. R-Squ	0.98937	

Model	GaussAmp	
Equation	y=y0+A*exp(-0.5*((x-xc)/w)^2)	
Plot	Peak1(D)	Peak2(D)
y0	124.19977 ± 10	124.19977 ± 10
xc	14887.10569 ±	18839.63748 ±
w	1345.25315 ± 4	1676.04098 ± 3
A	3944.40936 ± 1	6132.83391 ± 9
Reduced C	136256.78215	
R-Square (	0.95958	
Adj. R-Squa	0.95896	

Figure S2. The original fluorescence spectra of **NA1** in acetonitrile (a) and **NA2** in acetone (c) and acetonitrile (d). Blue, red and green lines show Gaussian fit.

Table S3. Wavelengths of absorption spectra maxima in solvents of different refractive indexes (n) and dielectric constants (ε) for **DPO**, **NA1** and **NA2**.

Solvent	**n**	**ε**	**λ_{ABS}, nm**		
			DPO	**NA1**	**NA2**
Nonafluorobutyl methyl ether (9FBME)	1.3	4	383	405	
Acetonitrile (ACN)	1.341	37.5	394	424	448
Diethyl ether (DEE)	1.3495	4.33	--	414	443
Pentane (Pen)	1.3547	1.84	392	403	444
Acetone (AC)	1.356	20.7	--	423	448
Ethyl acetate (EA)	1.3698	6.02	--	420	445
Dimethoxyethane (DME)	1.38	7.2	--	423	449
Decane (Dec)	1.4097	2	396	408	450
Cyclohexane (CyHex)	1.426	2.02	--	407	452
Chloroform (CHL)	1.442	4.81	--	429	--
Toluene (TOL)	1.4941	2.38	410	420	--

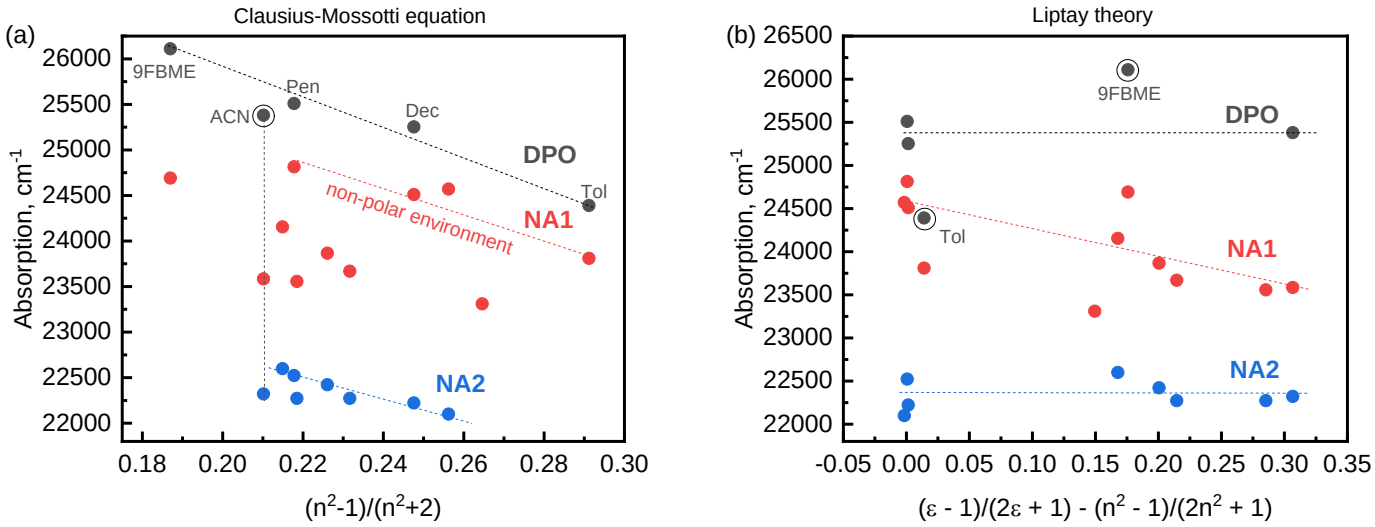

Figure S3. Wavenumbers of absorption spectra peaks versus solvents' parameters, expressed as Clausius-Mossotti equation (a) and Lippert parameter used in Liptay theory (b) for reference molecule 1,8-diphenyl-1,3,5,7-octatetraene (**DPO**) (black points) and studied compounds **NA1** (red points) and **NA2** (blue points) compounds.

The absorption spectra behaviour towards solvents' parameters were evaluated by employing Claussius-Mossotti and Liptay theory with Lippert parameter approaches for reference molecule 1,8-diphenyl-1,3,5,7-octatetraene (**DPO**) and both studied compounds **NA1** and **NA2**. First, the classic Claussius-Mossotti relationship of λ_{ABS} versus $(n^2-1)/(n^2+2)$ revealed that the absorption spectral position is sensitive to solvents' refractive index (Figure S3 a). In case of **NA2**, most of data points could be fitted linearly, except of results in acetone and acetonitrile, that are additionally affected by specific solvent-chromophore interaction. In case of **NA1**, large deviation from a linear fit was observed, suggesting different solvation in each solvent.

Next, the Liptay theory with Lippert parameter was exploited to account both, for dielectric constant and refractive index (Figure S3 b). Both, the reference molecule **DPO** and

studied molecule **NA2** show no pronounced changes of absorption spectral position on solvent's polarizability. According to Liptay equation[7] with Lippert parameter[8] $\Delta f = \frac{(\varepsilon-1)}{(2\varepsilon+1)} - \frac{(n^2-1)}{(2n^2+1)}$:

$$\vartheta_{ABS} = \frac{1}{4\pi\varepsilon_0}\mu_g\left(\mu_e^{FC} - \mu_g\right)\Delta f, \quad (6)$$

the almost zero solvatochromic slope of **NA2** (as well as **DPO**) suggests that ground (μ_g) and Franck-Condon (FC) excited state (μ_e^{FC}) dipole moments are roughly the same,[9] especially considering the non-zero ground state dipole moment for studied compounds (Table S2).

The case of **NA1** is more complex. The steric interaction between phenyl ring and naphthalimide determines a partially twisted ground state geometry. Different solvents may cause slightly different ground and FC excited state geometries that result in different response to solvents' orientation polarizability and thus, slight red-shift of absorption spectra. Thus, the scatter of data points is observed in Figure S3 a, while in Figure S3 b the trend of slight absorption spectra red-shift along with increased solvents' dielectric constant is seen.

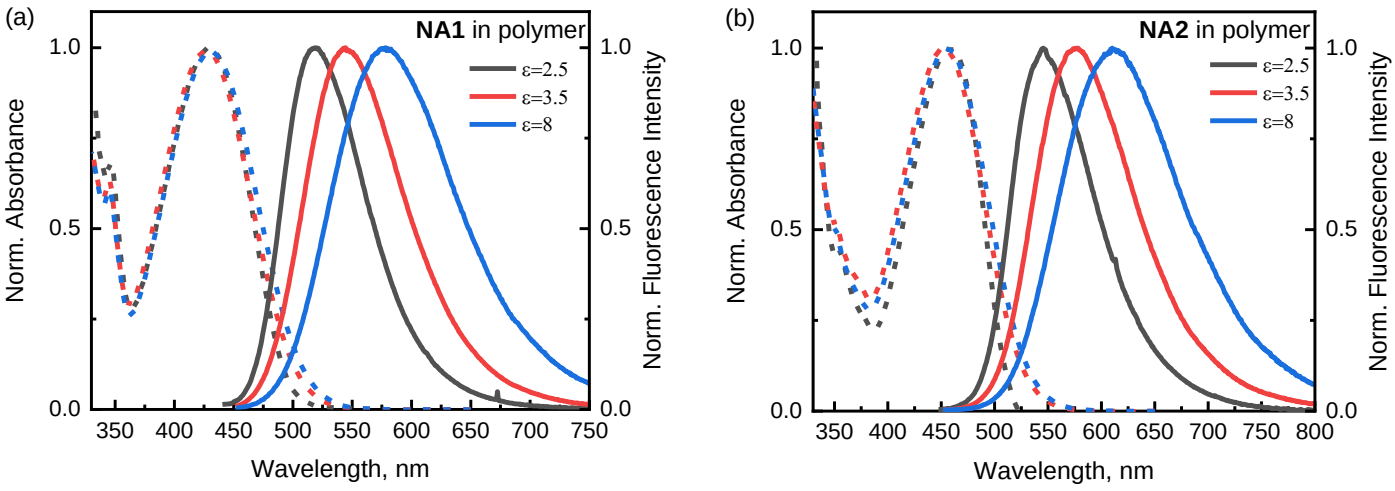

Figure S4. Normalized absorption and fluorescence spectra of **NA1** (a) and **NA2** (b) in polymers of different dielectric constants: 1 wt% PS (ε=2.5, black), 1 wt% PMMA (ε=3.5, red), and 1 wt% PMMA with 20 wt% CA (ε=8, blue).

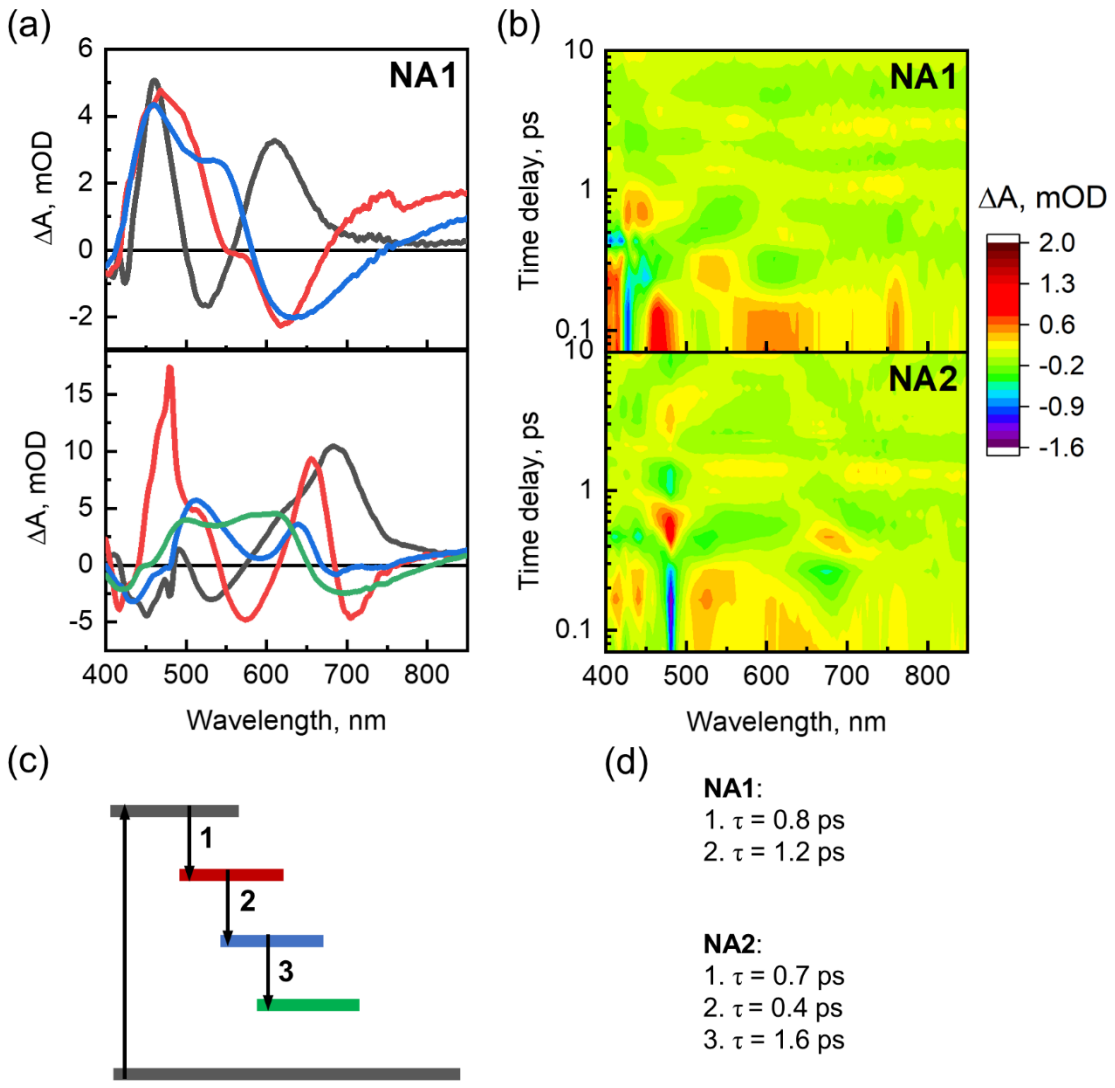

Figure S5. The evolution associated spectra (a) obtained by Global Analysis (GA) and the residuals showing the discrepancy between measured and fitted Transient Absorption experiment data (b) for **NA1** and **NA2** in ethyl acetate. The applied model to perform GA includes 3 compartments for **NA1** and 4 compartments for **NA2**. The excited state reaction rates are given in (d) for both of compounds.

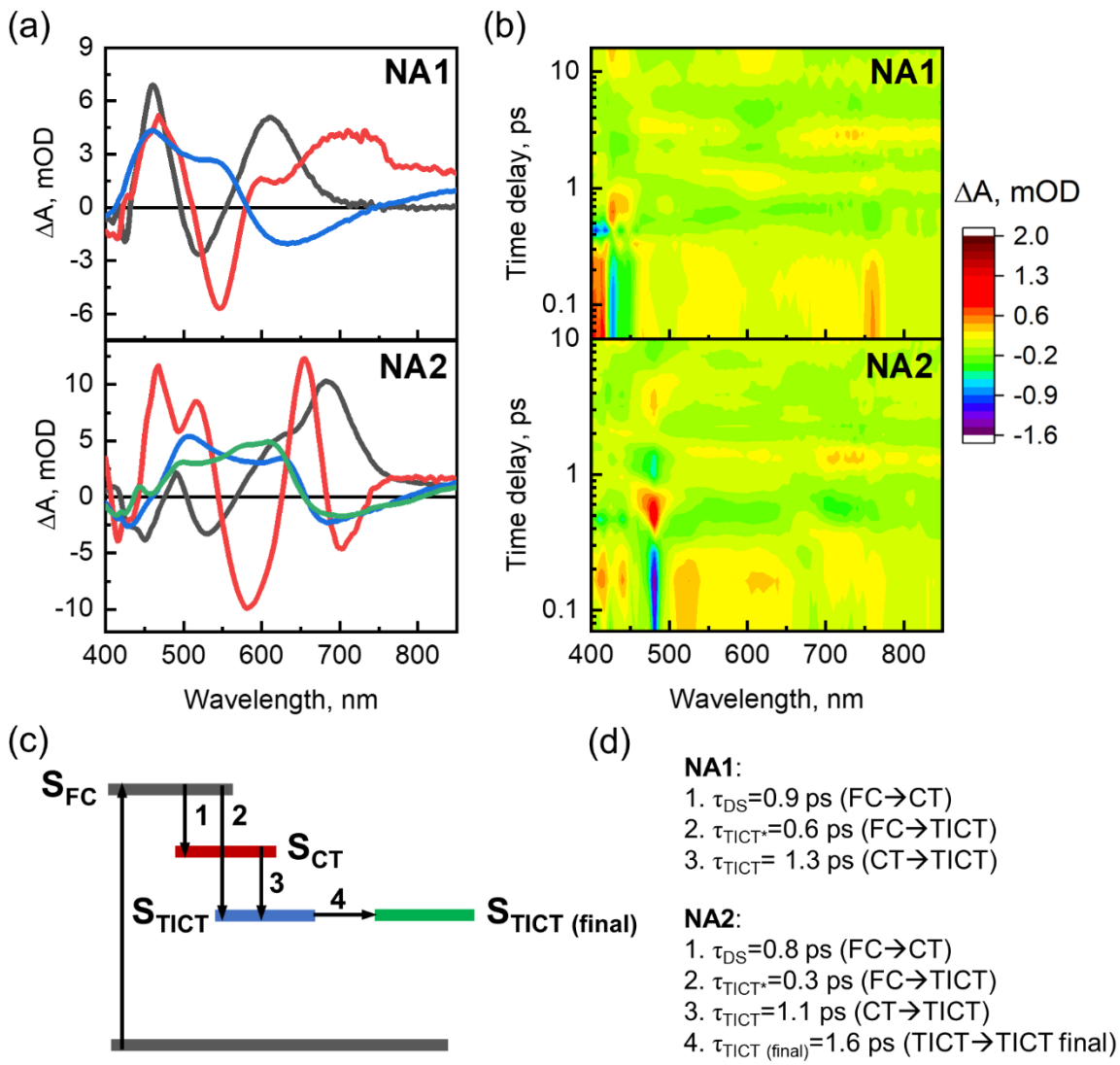

Figure S6. The decay associated spectra (a) obtained by Global Analysis (GA) and the residuals showing the discrepancy between measured and fitted Transient Absorption experiment data (b) for **NA1** and **NA2** in ethyl acetate. The applied model to perform GA includes excited Franck Condon state (S_{FC}), the excited solvated partially twisted/planar charge transfer state (S_{CT}), the excited twisted intramolecular charge transfer state (S_{TICT}) and final TICT state ($S_{TICT\ (final)}$) that was included only for **NA2**. The excited state reaction rates are given in (d) for both of compounds.

References

1 D. Gudeika, R. Lygaitis, V. Mimaitė, J. V. Grazulevicius, V. Jankauskas, M. Lapkowski and P. Data, *Dye. Pigment.*, 2011, **91**, 13–19.

2 K. Suzuki, A. Kobayashi, S. Kaneko, K. Takehira, T. Yoshihara, H. Ishida, Y. Shiina, S. Oishi and S. Tobita, *Phys. Chem. Chem. Phys.*, 2009, **11**, 9850.

3 H. Beens, H. Knibbe and A. Weller, *J. Chem. Phys.*, 2004, **47**, 1183.

4 P. A. Panchenko, A. N. Arkhipova, O. A. Fedorova, Y. V. Fedorov, M. A. Zakharko, D. E. Arkhipov and G. Jonusauskas, *Phys. Chem. Chem. Phys.*, 2017, **19**, 1244–1256.

5 J. B. . F. Frisch, M. J.; Trucks, G. W.; Schlegel, H. B.; Scuseria, G. E.; Robb, M. A.; Cheeseman, J. R.; Scalmani, G.; Barone, V.; Petersson, G. A.; Nakatsuji, H.; Li, X.; Caricato, M.; Marenich, A. V.; Bloino, J.; Janesko, B. G.; Gomper, *Gaussian, Inc., Wallingford CT*.

6 J. J. P. Stewart, *J. Mol. Model.*, 2013, **19**, 1–32.

7 W. Liptay, *Zeitschrift fur Naturforsch. - Sect. A J. Phys. Sci.*, 1965, **20**, 1441–1471.

8 E. Lippert, *Zeitschrift fur Naturforsch. - Sect. A J. Phys. Sci.*, 1955, **10**, 541–545.

9 H. El-Gezawy, W. Rettig and R. Lapouyade, *J. Phys. Chem. A*, 2006, **110**, 67–75.